Anatomical predictors of recovery from visual neglect after prism adaptation therapy

Marine Lunven[1,2,3,4], Gilles Rode[3,5], Clémence Bourlon[2,6], Christophe Duret[2], Raffaella Migliaccio[1], Emmanuel Chevrillon[7], Michel Thiebaut de Schotten[1,4*], Paolo Bartolomeo[1*].

1. *Inserm U 1127, CNRS UMR 7225, Sorbonne Universités, UPMC Univ Paris 06 UMR S 1127, Institut du Cerveau et de la Moelle épinière, ICM, Hôpital de la Pitié-Salpêtrière, F-75013, Paris, France.*
2. *Service de Médecine Physique et Réadaptation, Unité de Rééducation Neurologique CRF "Les Trois Soleils" Boissise le Roi, France*
3. *Inserm UMR_S 1028, CNRS UMR 5292; ImpAct, centre des neurosciences de Lyon, université Lyon-1, 16, avenue Lépine 69676 Bron, France*
4. *Brain connectivity and behaviour group, Institut du Cerveau et de la Moelle épinière, ICM, Hôpital de la Pitié-Salpêtrière, F-75013, Paris, France.*
5. *Service de médecine physique et réadaptation neurologique, hospital Henry-Gabrielle, hospices civils de Lyon, 20, route de Vourles, Saint-Genis-Laval, France*
6. *Hôpitaux de Saint Maurice, Saint Maurice, France*
7. *Clinique du Bourget, Le Bourget, France*

*contributed equally

Corresponding author: Paolo Bartolomeo, paolo.bartolomeo@gmail.com

Abstract

Visual neglect is a frequent and disabling consequence of right hemisphere damage. Previous evidence demonstrated a probable role of posterior callosal dysfunction in the chronic persistence of neglect signs. Prism adaptation is a non-invasive and convenient technique to rehabilitate chronic visual neglect, but it is not effective in all patients. Here we hypothesized that prism adaptation improves left neglect by facilitating compensation through the contribution of the left, undamaged hemisphere. To test this hypothesis, we assessed the relationship between prism adaptation effects, cortical thickness and white matter integrity in a group of 14 patients with unilateral right-hemisphere strokes and chronic visual neglect. Consistent with our hypothesis, patients who benefitted from prism adaptation had a thicker cortex in temporo-parietal, prefrontal and cingulate areas of the left, undamaged hemisphere. Additionally, these patients had higher microstructural integrity of the body and genu of the corpus callosum. These callosal regions connect temporo-parietal, sensorimotor and prefrontal areas. Thus, prism adaptation may ameliorate signs of left visual neglect by promoting the contribution of the left hemisphere to neglect compensation. These results support current hypotheses on the role of the healthy hemisphere in the compensation for stroke-induced, chronic neuropsychological deficits, and suggest that prism adaptation can foster this role by exploiting sensorimotor/prefrontal circuits for neglect compensation.

Highlights:

- Visual neglect is a disabling condition resulting from right hemisphere damage
- Prism adaptation is a promising therapy, but not all patients respond
- We assessed the anatomical predictors of patients' response to prism adaptation
- Study of cortical thickness and white matter integrity
- Importance of fronto-parietal networks in the left, healthy hemisphere for recovery
- Importance of callosal connections in the genu and body for recovery

Keywords: Visual neglect, prism adaptation, cortical thickness, fractional anisotropy, inter-hemispheric communication

1. Introduction

Cognitive rehabilitation after a vascular stroke is one of the main concerns of public health. Visual neglect is a frequent and disabling consequence of right hemisphere lesions (Heilman and Van Den Abell, 1980; Mesulam, 1981). Neglect patients are unable to pay attention to left-sided objects, with consequent loss of autonomy and poor functional outcome. At least 80% of patients with a right hemispheric stroke show signs of visual neglect in the acute stage (Azouvi et al., 2002). Impaired integration of attention-related processes within the right hemisphere (Corbetta and Shulman, 2011; Doricchi et al., 2008), as well as between the right and the left hemispheres (Bartolomeo et al., 2007; Heilman and Adams, 2003) contributes to neglect behaviour. About half of neglect patients still show signs of neglect one year or more after the stroke (Lunven et al., 2015), perhaps because posterior callosal dysfunction prevents attention-critical regions in the healthy hemisphere to access information processed by the damaged right hemisphere (Lunven et al., 2015).

Prism adaptation is a convenient technique to improve the ratio of recovering patients, because it is totally non-invasive and easy to administer (Rossetti et al., 1998; Yang et al., 2013). Patients wear prismatic goggles, which displace rightwards the whole visual field; this induces an initial rightward bias in manual reaching movements, which disappears after a few trials. After removal of the prisms, reaching is initially deviated towards the left, neglected side, and neglect signs can disappear. Unfortunately, neglect does not improve in all treated patients (Luauté et al., 2006; Rode et al., 2015; Rousseaux et al., 2006; Saj et al., 2013), for unknown reasons (Barrett et al., 2012; Chokron et al., 2007).

Drawing on our previous evidence suggesting a role for posterior callosal dysfunction in the chronic persistence of neglect (Lunven et al., 2015), here we hypothesized that prism

adaptation might improve neglect by facilitating compensation through the contribution of the left, undamaged hemisphere. To test this hypothesis, we assessed the relationship between prism adaptation effects, cortical thickness and white matter integrity in a group of 14 patients with unilateral right-hemisphere stroke and chronic visual neglect.

2. Methods

2.1. Subjects

This study has been approved by the local Ethics Committee (CPP C10-48). A group of 14 patients with a single right hemisphere haemorrhagic or ischemic stroke, which had occurred at least 3 months before testing, and stable signs of left visual neglect, participated to our study. None of the patients had prior history of neurological disease or psychiatric disorders. Visual neglect was assessed by using six paper-and-pencil tasks: letter cancellation (Mesulam, 1985), copy of a linear drawing of a landscape (Gainotti et al., 1989), drawing from memory of a daisy (Rode et al., 2001); text reading (Azouvi et al., 2006), bisection of five 20-cm horizontal lines (Azouvi et al., 2006) and landmark task (Harvey and Milner, 1999). All patients received neglect tests on three occasions: (1) the day before prism adaptation, (2) two hours before prism adaptation and (3) soon after prism adaptation. For each assessment, a neglect severity score was computed as previously reported (Lunven et al., 2015), by using the percentage of left omissions for letter cancellation, drawing and reading tasks, the percentage of rightwards deviation for line bisection, and the percentage of left lateralised errors for the landmark task.

2.3. Prism adaptation

Following a previously described procedure (Rossetti et al., 1998), patients were asked to wear prismatic goggles that shifted the visual field 10 degrees towards the right. While

wearing prisms, patients were required to make, as quickly as possible, a series of approximately 100 pointing responses with the right hand towards left and right targets. The starting point of the hand was occluded to ensure optimal adaptation. The head of the patients was aligned with their body sagittal axis. Before and after the prism adaptation session, eye blinded patients were asked to point ten times straight-ahead with their right arm. The percentage of neglect improvement after prism adaptation was quantified using the following formula: (neglect score post-prism adaptation – neglect score pre-prism adaptation) / (neglect severity score pre-prism adaptation).

We split patients into two groups according to their recovery score. Patients with a recovery score above 20% were affected to the "high-responder" group (N=8), whereas patients with a recovery score below 20% were considered as "low-responders" (N=6). This classification was in good agreement with clinical assessment of patients' evolution (see Table 1).

2.4. Imaging data acquisition and lesion analysis

2.4.1. Data acquisition

An axial three-dimensional MPRAGE dataset covering the whole head was acquired for each participant (176 slices, voxel resolution = 1 × 1 × 1 mm, TE = 3 msec, TR = 2300 msec, flip angle = 9°) on a Siemens 3 T VERIO TIM system equipped with a 32-channel head coil.

Additionally, a total of 70 near-axial slices was acquired using an acquisition sequence fully optimized for tractography of DWI, which provided isotropic (2 × 2 × 2 mm) resolution and coverage of the whole head. The acquisition was peripherally-gated to the cardiac cycle (Conturo et al., 1995; Jones et al., 2002; Turner et al., 1990) with an echo time (TE) = 85 msec. We used a repetition time (TR) equivalent to 24 RR intervals assuming that

spins would have fully relaxed before the repetition. At each slice location, six images were acquired with no diffusion gradient applied. Additionally, 60 diffusion-weighted images were acquired, in which gradient directions were uniformly distributed in space. The diffusion weighting was equal to a *b*-value of 1500 sec mm^{-2}.

2.4.2. Study of grey matter

Abnormal tissues were delineated on the T1-weighed images using MRIcroN for each patient (Rorden and Brett, 2000). T1-weighted images were normalized in the Montreal Neurological Institute (MNI) space (http://www.mni.mcgill.ca/) using rigid and elastic deformation tools provided in the software package Statistical Parametric Mapping 8 (SPM8, http://www.fil.ion.ucl.ac.uk/spm). Deformation was applied to the whole brain except for the voxels contained in the lesion mask, in order to avoid deformation of the lesioned tissue (Brett et al., 2001; Volle et al., 2008). Finally, the lesion were carefully drawn in the MNI space by an expert neuropsychologist (ML) and checked by an expert neurologist (RM). Subsequently, lesions were overlapped for each of the high-responders and low-responders group.

2.4.3. Cortical Thickness preprocessing

Cortical thickness was derived from the T1-weighted imaging dataset using a registration-based method (Diffeomorphic Registration based Cortical Thickness, DiReCT) (Das et al., 2009) optimised in BCBtoolkit (http://toolkit.bcblab.com) for patients with a brain lesion (Foulon et al.) This approach has good scan-rescan repeatability and good neurobiological validity as it can predict with a high statistical power the age and gender of the participants (Tustison et al., 2014). These data were then normalized to MNI space with the previous deformation estimated to normalize the T1-weighted imaging dataset.

2.4.4. Study of white matter

From pairs of images with distortions going in opposite directions the susceptibility-induced off-resonance field was estimated by using a previously described method (Andersson et al., 2003), as implemented in FSL (Smith et al., 2004), and the two images were combined into a single corrected one. Next, we extracted brain using BET implemented in FSL and we corrected diffusion datasets simultaneously for motion and geometrical distortions by using ExploreDTI http://www.exploredti.com (Leemans and Jones, 2009). The tensor model was fitted to the data by using the Levenberg-Marquardt non-linear regression (Marquardt, 1963). Fractional anisotropy (FA) maps were extracted for each subject by using the function "extract stuff", which is part of the ExploreDTI software package.

FA maps were further processed using Tract-Based-Spatial Statistics (TBSS) implemented in FSL software [http://fsl.fmrib.ox.ac.uk/fsl/fslwiki/TBSS, (Smith et al., 2006)]. TBSS register FA maps and extract their core (FA>0.2) of the white matter maps and because we studied stroke patients, we changed some parameters in the original TBSS preprocessing. During the non-linearly registration of FA maps to an averaged FA template into 1x1x1mm MNI-152 standard space using FNIRT, lesion mask for each patient was used. Next, an average FA map was created and a skeleton map representing the center of the white matter (FA > 0.2) common to all patients computed. Finally, the registered FA maps were projected into the skeleton.

2.4.5. Statistical analysis

We statistically compared FA and cortical thickness values between low-responder and high-responder patients. Visual field defects and lesion volume were included as co-variables of non-interest. Lesioned voxels were excluded from these analyses. Statistical differences were assessed using the function "Randomise"

(http://fsl.fmrib.ox.ac.uk/fsl/fslwiki/Randomise/) implemented in FSL, with 5,000 random permutation tests and a Threshold-Free Cluster Enhancement option (Smith and Nichols, 2009). Results were adjusted for family wise error (FWE) corrections for multiple comparisons and thresholded at $p<0.05$.

Second, we conducted a regression analysis including all the 14 patients in order to identify a dimensional relationship between the fractional anisotropy, the cortical thickness and the percentage of improvement after prism adaptation. Lesion volume and visual field defect were also included as continuous co-variables of non-interest, in order to avoid spurious differences. Again, statistical difference were calculated using the function "Randomise" implemented in FSL, with 5,000 random permutation tests and a Threshold-Free Cluster Enhancement option (Smith and Nichols, 2009). Results were adjusted for FWE corrections for multiple comparisons and thresholded at $p<0.05$.

For each statistical analysis, effect sizes were calculated using gpower (http://www.gpower.hhu.de/en.html).

3. Results

3.1. Behavioural results

There was no significant difference between neglect severity scores assessed the day before prism adaptation and two hours before prism adaptation (first session: mean score 29.08, SD 20.33; second session: mean score 30.81, SD 21.57; Wilcoxon Signed-Ranks Test, $Z=-0.345$, $p=0.73$), thus suggesting a generally stable level of performance before prism adaptation. Prism adaptation induced a sensorimotor adaptation in all patients, who deviated rightward before PA (6.47 degrees ± 3.51) and towards the left after prism adaptation (-1.95 degrees SD, 2.83) ($Z=-3.234$ $p=0.001$). There was no correlation between neglect recovery scores and

prism adaptation effect on the straight-ahead task, consistent with previous results (Pisella et al., 2002).

Table 1 reports patients' demographic, clinical and neuropsychological data. High-responder and low-responder patients had similar age (Mann-Whitney U=34; p=0.23), with high-responders being numerically older (mean, 69.62 years, SD 6.82) than low-responders (59.50 years, SD 13.47). Low-responders had numerically larger lesion volumes, but the difference was not significant (U=14; p=0.23). Low- and high-responders had similar neglect severity scores before prism adaptation (U=28; p=0.66). Homonymous hemianopia was present in three low-responders and in three high-responders.

As expected, high-responder patients demonstrated a statistically reliable improvement on visuospatial tests after prism adaptation (Wilcoxon Signed-Ranks Test, Z=-2.52; p=0.012), while this was not the case for the low-responder subgroup (Z=-0.67; p=0.50). In particular, high-responders detected more left items in letter cancellation (Z=-2.39, p=0.017), drew more left-sided items in landscape copy (Z= -2.06, p=0.039) and in daisy drawing (Z=-2.24; p=0.025), and had a more symmetrical performance when bisecting lines (Z=-2.240; p=0.025). However, prism adaptation did not significantly impact performance on the reading task (Z=-1.604; p=0.11) and on the Landmark task (Z=-0.365; p=0.715).

3.2. Lesion analysis

The maximum lesion overlap was centred in the right fronto-parietal white matter in both patient subgroups (Figure 1.1). In low-responders, damage also involved the supramarginal and angular gyri of the inferior parietal lobule. Lesion subtraction (Figure 1.2) between low and high responders showed mostly parietal regions, including the inferior parietal lobule, the

postcentral gyrus, but also frontal regions with the precentral gyrus, the superior frontal lobe, the orbito-frontal cortex, and the fronto-parietal white matter.

3.3. Cortical thickness

Group comparison by using the FSL function "randomise" showed no significant results. However, regression analysis between cortical thickness and recovery scores revealed three significant clusters in the left, undamaged hemisphere (Figure 2 and Table 2). The first cluster involved the perisylvian region, including the surface of the inferior parietal lobule, the three temporal gyri, somatosensory areas and the prefrontal cortex, with a medium effect size (0.26). The second cluster was located in the posterior part of the superior temporal sulcus. The third and last cluster was situated in the anterior portion of the left inferior temporal sulcus. These clusters had large effect sizes (>0.60).

3.4. White matter analyses

FA group comparison revealed a significant decrease in low-responders as compared to high-responders in three clusters, all with large effect sizes (>0.80) (Figure 3, Table 3). The first cluster was located in the body of the corpus callosum. The second cluster encompassed the genu of the corpus callosum. The third cluster identified a portion of the genu of the corpus callosum within the left, undamaged hemisphere. We used Tractotron software included in the Brain Connectivity and Behaviour toolkit (http://toolkit.bcblab.com) to visualize in ten healthy subjects the white matter tracts passing through the voxels showing a significant difference between the patient subgroups. The analysis revealed that the fibres running through the voxels in the first cluster mostly connect sensorimotor areas (Figure 4). These areas include the primary somato-sensory cortex, the primary motor cortex, the associative somato-sensorial cortex, the premotor cortex, as well as several prefrontal areas. Additional

regions connected by the first cluster were localised in the temporal lobe (middle and superior gyri), and in the parietal lobe (supramarginal gyrus, precuneus and superior parietal lobule). The second and the third clusters connected prefrontal areas. Regression analyses between FA values and percentage of improvement after prism adaptation did not disclose any significant correlations.

4. Discussion

In this study, we followed up a group of patients with chronic visual neglect, before and after prism adaptation. We used advanced neuroimaging techniques to identify the anatomical predictors of neglect patients' response to prism adaptation. First, cortical thickness analyses indicated a significant contribution of the left, undamaged hemisphere. Second, diffusion weighted imaging demonstrated an important role for inter-hemispheric connections in PA efficiency.

In the left, healthy hemisphere, cortical thickness analyses revealed a significant involvement of the temporo-parietal areas in the prism adaptation cognitive effect. Surprisingly, these regions also match areas contributing to right visual neglect after a stroke in the left hemisphere (Beume et al., 2016), and mirror classical areas reported as involved in left visual neglect after a stroke in the right hemisphere (Corbetta and Shulman, 2011). This may suggest that the left temporo-parietal junction is predisposed to compensate for left visual neglect (Bartolomeo and Thiebaut de Schotten, 2016). Consistent with this hypothesis, previous studies reported an involvement of the left hemisphere in the recovery of neglect after prism adaptation therapy (Levin et al., 2009; Luauté et al., 2006; Saj et al., 2013).

Two possibilities can explain the difference in cortical thickness in the controlesional hemisphere. First, some individual brains may have a better predisposition to recover than

others (i.e. a thicker left temporo-parietal junction). These findings would therefore mirror analogous results in the domain of recovery from aphasia, which appears to be promoted by stronger language structures in the right hemisphere (Forkel et al., 2014; Xing et al., 2016). An alternative hypothesis might be that diaschisis and disconnection may have induced secondary atrophy in remote cortices (Cheng et al., 2015; Foulon et al., 2017). This would be consistent with previous reports suggesting that bilateral diffuse tissue loss may occur in individuals with chronic stroke (Gauthier et al., 2012; Kraemer et al., 2004). Thus, premorbid atrophy in left temporo-parietal areas might hamper cognitive effects related to PA after a stroke in the right hemisphere (see Levine et al., 1986). Future longitudinal studies comparing acute to chronic stages of vascular strokes will be necessary to adjudicate between these two possibilities.

In order to assess whether response to prism adaptation and cortical thickness in remote cortices was due to a brain disconnection, we contrasted FA measures between low- and high responder. Low-responder patients had a selective decrease of callosal FA in the body and genu of the corpus callosum, which mainly connect sensorimotor and prefrontal areas (Catani & Thiebaut de Schotten 2012). This result suggests that prism adaptation improves left neglect by allowing left-hemisphere attentional networks to access information processed by the lesioned right hemisphere, through the callosal body and genu. An implication of prefrontal circuits in neglect compensation has been hypothesized on the basis of behavioural evidence (Bartolomeo, 2000, 1997), and recently confirmed by electrophysiological measures (Takamura et al., 2016). Also consistent with our results, cathodal transcranial direct current stimulation applied over the left posterior parietal cortex interfered with the beneficial effect of prism adaptation on neglect (Làdavas et al., 2015).

Limitations of the study

The principal limitation of this study is that only 14 patients could be followed up before and after prism adaptation, and the design of the study required this sample to be further subdivided in two subgroups (high- and low-responders). We note, however, first, that the sample size was sufficient to obtain significant results with TBSS, which is a notoriously conservative technique. Second, a power analysis indicated a medium to large effect size for the left temporo-parietal junction, temporal lobe and white matter findings. Third, we found evidence consistent with previous studies in the lesion subtraction analysis, which showed differences between high-responders and low-responders in the right supramarginal and postcentral gyri, together with frontal areas and fronto-parietal white matter. This finding is in broad agreement with previous similar evidence that lesions to the right hemisphere posterior parietal cortex and the superior frontal gyrus (Rousseaux et al., 2006), the infero-posterior parietal cortex (Luauté et al., 2006), the intra-parietal sulcus, the white matter around the inferior parietal lobule, the middle frontal gyrus (Sarri et al., 2008), the occipital lobe (Serino et al., 2006) and the right cerebellum (patient 5 in (Saj et al., 2013)) hampered prism adaptation efficiency. Thus, our patient population appears to be representative of the general lesional patterns in chronic neglect patients.

Conclusions and perspectives

In conclusion, our results confirm the importance of the left, healthy hemisphere (Bartolomeo and Thiebaut de Schotten, 2016) and of inter-hemispheric connections in recovery from neglect (Lunven et al., 2015). Specifically, left hemisphere regions homologues to the fronto-parietal attention networks in the right hemisphere (Corbetta and Shulman, 2002), as well as callosal pathways passing through the body and the genu, appear to be critical for compensation of neglect signs after a single prism adaptation session. It remains to be seen

whether or not more prolonged rehabilitation programmes using prism adaptation (Frassinetti et al., 2002) require similar anatomical constraints. The identification of anatomical predictors of response to different, labour-intensive rehabilitation strategies may ultimately enable clinicians to select and tailor the appropriate treatment to the specific needs of the individual patient. Finally, the relationship between recovery and controlesional cortical thickness suggests potential targets for future therapeutic interventions.

Acknowledgments

We would like to thank Cécile Coste, Fanny Lagneau, Emilie Monnot and Marika Urbanski for help with patient recruitment. The research leading to these results has received funding from a CIFRE grant to ML, from an AP-HP translational research grant to PB, from the ANR "Phenotypes" ANR-13-JSV4-0001-01 to MTS and from the program "Investissements d'Avenir" ANR-10-IAIHU-06.

References

Andersson, J.L.R., Skare, S., Ashburner, J., 2003. How to correct susceptibility distortions in spin-echo echo-planar images: application to diffusion tensor imaging. NeuroImage 20, 870–888. doi:10.1016/S1053-8119(03)00336-7

Azouvi, P., Bartolomeo, P., Beis, J.-M., Perennou, D., Pradat-Diehl, P., Rousseaux, M., 2006. A battery of tests for the quantitative assessment of unilateral neglect. Restor. Neurol. Neurosci. 24, 273–285.

Azouvi, P., Samuel, C., Louis-Dreyfus, A., Bernati, T., Bartolomeo, P., Beis, J.-M., Chokron, S., Leclercq, M., Marchal, F., Martin, Y., De Montety, G., Olivier, S., Perennou, D., Pradat-Diehl, P., Prairial, C., Rode, G., Siéroff, E., Wiart, L., Rousseaux, M., French Collaborative Study Group on Assessment of Unilateral Neglect (GEREN/GRECO), 2002. Sensitivity of clinical and behavioural tests of spatial neglect after right hemisphere stroke. J. Neurol. Neurosurg. Psychiatry 73, 160–166.

Barrett, A.M., Goedert, K.M., Basso, J.C., 2012. Prism adaptation for spatial neglect after stroke: translational practice gaps. Nat. Rev. Neurol. 8, 567–577. doi:10.1038/nrneurol.2012.170

Bartolomeo, P., 2000. Inhibitory processes and spatial bias after right hemisphere damage. Neuropsychol. Rehabil. 10, 511–526. doi:10.1080/09602010050143577

Bartolomeo, P., 1997. The novelty effect in recovered hemineglect. Cortex 33, 323–332.

Bartolomeo, P., Thiebaut de Schotten, M., 2016. Let thy left brain know what thy right brain doeth: Inter-hemispheric compensation of functional deficits after brain damage. Neuropsychologia 93, 407–412. doi:10.1016/j.neuropsychologia.2016.06.016

Bartolomeo, P., Thiebaut de Schotten, M., Doricchi, F., 2007. Left unilateral neglect as a disconnection syndrome. Cereb. Cortex N. Y. N 1991 17, 2479–2490. doi:10.1093/cercor/bhl181

Beume, L.-A., Martin, M., Kaller, C.P., Klöppel, S., Schmidt, C.S.M., Urbach, H., Egger, K., Rijntjes, M., Weiller, C., Umarova, R.M., 2016. Visual neglect after left-hemispheric lesions: a voxel-based lesion–symptom mapping study in 121 acute stroke patients. Exp. Brain Res. 1–13. doi:10.1007/s00221-016-4771-9

Brett, M., Leff, A.P., Rorden, C., Ashburner, J., 2001. Spatial normalization of brain images with focal lesions using cost function masking. NeuroImage 14, 486–500. doi:10.1006/nimg.2001.0845

Cheng, B., Schulz, R., Bönstrup, M., Hummel, F.C., Sedlacik, J., Fiehler, J., Gerloff, C., Thomalla, G., 2015. Structural plasticity of remote cortical brain regions is determined by connectivity to the primary lesion in subcortical stroke. J. Cereb. Blood Flow Metab. Off. J. Int. Soc. Cereb. Blood Flow Metab. 35, 1507–1514. doi:10.1038/jcbfm.2015.74

Chokron, S., Dupierrix, E., Tabert, M., Bartolomeo, P., 2007. Experimental remission of unilateral spatial neglect. Neuropsychologia 45, 3127–3148. doi:10.1016/j.neuropsychologia.2007.08.001

Conturo, T.E., McKinstry, R.C., Aronovitz, J.A., Neil, J.J., 1995. Diffusion MRI: precision, accuracy and flow effects. NMR Biomed. 8, 307–332.

Corbetta, M., Shulman, G.L., 2011. Spatial neglect and attention networks. Annu. Rev. Neurosci. 34, 569–599. doi:10.1146/annurev-neuro-061010-113731

Corbetta, M., Shulman, G.L., 2002. Control of goal-directed and stimulus-driven attention in the brain. Nat. Rev. Neurosci. 3, 201–215. doi:10.1038/nrn755

Das, S.R., Avants, B.B., Grossman, M., Gee, J.C., 2009. Registration based cortical thickness measurement. NeuroImage 45, 867–879. doi:10.1016/j.neuroimage.2008.12.016

Doricchi, F., Thiebaut de Schotten, M., Tomaiuolo, F., Bartolomeo, P., 2008. White matter (dis)connections and gray matter (dys)functions in visual neglect: gaining insights into the brain networks of spatial awareness. Cortex 44, 983–995. doi:10.1016/j.cortex.2008.03.006

Forkel, S.J., Thiebaut de Schotten, M., Dell'Acqua, F., Kalra, L., Murphy, D.G.M., Williams, S.C.R., Catani, M., 2014. Anatomical predictors of aphasia recovery: a tractography study of bilateral perisylvian language networks. Brain J. Neurol. 137, 2027–2039. doi:10.1093/brain/awu113

Foulon, C., Cerliani, L., Kinkingnehun, S., Levy, R., Rosso, C., Urbanski, M., Volle, E., Schotten, M.T. de, 2017. Advanced Lesion Symptom Mapping Analyses And Implementation As BCBtoolkit. bioRxiv 133314. doi:10.1101/133314

Frassinetti, F., Angeli, V., Meneghello, F., Avanzi, S., Làdavas, E., 2002. Long-lasting amelioration of visuospatial neglect by prism adaptation. Brain J. Neurol. 125, 608–623.

Gainotti, G., D'Erme, P., de Bonis, C., 1989. [Clinical aspects and mechanisms of visual-spatial neglect]. Rev. Neurol. (Paris) 145, 626–634.

Gauthier, L.V., Taub, E., Mark, V.W., Barghi, A., Uswatte, G., 2012. Atrophy of spared gray matter tissue predicts poorer motor recovery and rehabilitation response in chronic stroke. Stroke 43, 453–457. doi:10.1161/STROKEAHA.111.633255

Harvey, M., Milner, A.D., 1999. Residual perceptual distortion in "recovered" hemispatial neglect. Neuropsychologia 37, 745–750.

Heilman, K.M., Adams, D.J., 2003. Callosal neglect. Arch. Neurol. 60, 276–279.

Heilman, K.M., Van Den Abell, T., 1980. Right hemisphere dominance for attention: the mechanism underlying hemispheric asymmetries of inattention (neglect). Neurology 30, 327–330.

Jones, D.K., Griffin, L.D., Alexander, D.C., Catani, M., Horsfield, M.A., Howard, R., Williams, S.C.R., 2002. Spatial normalization and averaging of diffusion tensor MRI data sets. NeuroImage 17, 592–617.

Kraemer, M., Schormann, T., Hagemann, G., Qi, B., Witte, O.W., Seitz, R.J., 2004. Delayed shrinkage of the brain after ischemic stroke: preliminary observations with voxel-guided morphometry. J. Neuroimaging Off. J. Am. Soc. Neuroimaging 14, 265–272. doi:10.1177/1051228404264950

Làdavas, E., Giulietti, S., Avenanti, A., Bertini, C., Lorenzini, E., Quinquinio, C., Serino, A., 2015. a-tDCS on the ipsilesional parietal cortex boosts the effects of prism adaptation treatment in neglect. Restor. Neurol. Neurosci. 33, 647–662. doi:10.3233/RNN-140464

Leemans, A., Jones, D.K., 2009. The B-matrix must be rotated when correcting for subject motion in DTI data. Magn. Reson. Med. Off. J. Soc. Magn. Reson. Med. Soc. Magn. Reson. Med. 61, 1336–1349. doi:10.1002/mrm.21890

Levin, M.F., Kleim, J.A., Wolf, S.L., 2009. What Do Motor "Recovery" and "Compensation" Mean in Patients Following Stroke? Neurorehabil. Neural Repair 23, 313–319. doi:10.1177/1545968308328727

Levine, D.N., Warach, J.D., Benowitz, L., Calvanio, R., 1986. Left spatial neglect: effects of lesion size and premorbid brain atrophy on severity and recovery following right cerebral infarction. Neurology 36, 362–366.

Luauté, J., Michel, C., Rode, G., Pisella, L., Jacquin-Courtois, S., Costes, N., Cotton, F., le Bars, D., Boisson, D., Halligan, P., Rossetti, Y., 2006. Functional anatomy of the therapeutic effects of prism adaptation on left neglect. Neurology 66, 1859–1867. doi:10.1212/01.wnl.0000219614.33171.01

Lunven, M., Thiebaut De Schotten, M., Bourlon, C., Duret, C., Migliaccio, R., Rode, G., Bartolomeo, P., 2015. White matter lesional predictors of chronic visual neglect: a longitudinal study. Brain J. Neurol. 138, 746–760. doi:10.1093/brain/awu389

Marquardt, D.W., 1963. An Algorithm for Least-Squares Estimation of Nonlinear Parameters. J. Soc. Ind. Appl. Math. 11, 431–441. doi:10.2307/2098941

Mesulam, M.-M., 1985. Principles of Behavioral Neurology. Davis.

Mesulam, M.M., 1981. A cortical network for directed attention and unilateral neglect. Ann. Neurol. 10, 309–325. doi:10.1002/ana.410100402

Pisella, L., Rode, G., Farnè, A., Boisson, D., Rossetti, Y., 2002. Dissociated long lasting improvements of straight-ahead pointing and line bisection tasks in two hemineglect patients. Neuropsychologia 40, 327–334.

Rode, G., Lacour, S., Jacquin-Courtois, S., Pisella, L., Michel, C., Revol, P., Alahyane, N., Luauté, J., Gallagher, S., Halligan, P., Pélisson, D., Rossetti, Y., 2015. Long-term sensorimotor and therapeutical effects of a mild regime of prism adaptation in spatial neglect. A double-blind RCT essay. Ann. Phys. Rehabil. Med. 58, 40–53. doi:10.1016/j.rehab.2014.10.004

Rode, G., Rossetti, Y., Boisson, D., 2001. Prism adaptation improves representational neglect. Neuropsychologia 39, 1250–1254.

Rorden, C., Brett, M., 2000. Stereotaxic display of brain lesions. Behav. Neurol. 12, 191–200.

Rossetti, Y., Rode, G., Pisella, L., Farné, A., Li, L., Boisson, D., Perenin, M.T., 1998. Prism adaptation to a rightward optical deviation rehabilitates left hemispatial neglect. Nature 395, 166–169. doi:10.1038/25988

Rousseaux, M., Bernati, T., Saj, A., Kozlowski, O., 2006. Ineffectiveness of prism adaptation on spatial neglect signs. Stroke J. Cereb. Circ. 37, 542–543. doi:10.1161/01.STR.0000198877.09270.e8

Saj, A., Cojan, Y., Vocat, R., Luauté, J., Vuilleumier, P., 2013. Prism adaptation enhances activity of intact fronto-parietal areas in both hemispheres in neglect patients. Cortex J. Devoted Study Nerv. Syst. Behav. 49, 107–119. doi:10.1016/j.cortex.2011.10.009

Sarri, M., Greenwood, R., Kalra, L., Papps, B., Husain, M., Driver, J., 2008. Prism adaptation aftereffects in stroke patients with spatial neglect: pathological effects on subjective straight ahead but not visual open-loop pointing. Neuropsychologia 46, 1069–1080. doi:10.1016/j.neuropsychologia.2007.11.005

Serino, A., Angeli, V., Frassinetti, F., Làdavas, E., 2006. Mechanisms underlying neglect recovery after prism adaptation. Neuropsychologia 44, 1068–1078. doi:10.1016/j.neuropsychologia.2005.10.024

Smith, S.M., Jenkinson, M., Johansen-Berg, H., Rueckert, D., Nichols, T.E., Mackay, C.E., Watkins, K.E., Ciccarelli, O., Cader, M.Z., Matthews, P.M., Behrens, T.E.J., 2006. Tract-based spatial statistics: voxelwise analysis of multi-subject diffusion data. NeuroImage 31, 1487–1505. doi:10.1016/j.neuroimage.2006.02.024

Smith, S.M., Jenkinson, M., Woolrich, M.W., Beckmann, C.F., Behrens, T.E.J., Johansen-Berg, H., Bannister, P.R., De Luca, M., Drobnjak, I., Flitney, D.E., Niazy, R.K., Saunders, J., Vickers, J., Zhang, Y., De Stefano, N., Brady, J.M., Matthews, P.M., 2004. Advances in functional and structural MR image analysis and implementation as FSL. NeuroImage 23, Supplement 1, S208–S219. doi:10.1016/j.neuroimage.2004.07.051

Smith, S.M., Nichols, T.E., 2009. Threshold-free cluster enhancement: addressing problems of smoothing, threshold dependence and localisation in cluster inference. NeuroImage 44, 83–98. doi:10.1016/j.neuroimage.2008.03.061

Takamura, Y., Imanishi, M., Osaka, M., Ohmatsu, S., Tominaga, T., Yamanaka, K., Morioka, S., Kawashima, N., 2016. Intentional gaze shift to neglected space: a compensatory

strategy during recovery after unilateral spatial neglect. Brain J. Neurol. doi:10.1093/brain/aww226

Turner, R., Le Bihan, D., Maier, J., Vavrek, R., Hedges, L.K., Pekar, J., 1990. Echo-planar imaging of intravoxel incoherent motion. Radiology 177, 407–414. doi:10.1148/radiology.177.2.2217777

Tustison, N.J., Cook, P.A., Klein, A., Song, G., Das, S.R., Duda, J.T., Kandel, B.M., van Strien, N., Stone, J.R., Gee, J.C., Avants, B.B., 2014. Large-scale evaluation of ANTs and FreeSurfer cortical thickness measurements. NeuroImage 99, 166–179. doi:10.1016/j.neuroimage.2014.05.044

Volle, E., Kinkingnéhun, S., Pochon, J.-B., Mondon, K., Thiebaut de Schotten, M., Seassau, M., Duffau, H., Samson, Y., Dubois, B., Levy, R., 2008. The functional architecture of the left posterior and lateral prefrontal cortex in humans. Cereb. Cortex N. Y. N 1991 18, 2460–2469. doi:10.1093/cercor/bhn010

Xing, S., Lacey, E.H., Skipper-Kallal, L.M., Jiang, X., Harris-Love, M.L., Zeng, J., Turkeltaub, P.E., 2016. Right hemisphere grey matter structure and language outcomes in chronic left hemisphere stroke. Brain J. Neurol. 139, 227–241. doi:10.1093/brain/awv323

Yang, N.Y.H., Zhou, D., Chung, R.C.K., Li-Tsang, C.W.P., Fong, K.N.K., 2013. Rehabilitation Interventions for Unilateral Neglect after Stroke: A Systematic Review from 1997 through 2012. Front. Hum. Neurosci. 7, 187. doi:10.3389/fnhum.2013.00187

Table 1: Demographical and clinical characteristics of patients, with their performance on visuospatial tests before and after prism adaptation.

	High-Responder group N=8 mean (SD)		**Low-Responder group** N=6 mean (SD)		
Descriptive data					
Age (years)	69.62 (6.82)		59.5 (13.47)		p=0.089
Education	12.25 (3.65)		12 (2.82)		p=0.895
Lesion volume (cm^3)	106.53 (110,60)		228.98 (183,21)		p=0.145
Lesion-testing delay (days)	341.40 (340.59)		816.33 (484.29)		p=0.051
Motor deficit (number of patients)	4		3		
Visual field defect (number of patients)	3		3		
Neuropsychological results					
MMSE	27.00 (1.69)		26.83 (2.40)		p=0.881
Recovery rate (%)	36.29 (15.36)		-1.60 (22.18)		**p<0.01**
	Pre	**Post**	**Pre**	**Post**	
Neglect severity global score (%)	32.38 (20,10)	21.64 (16.69)	32.18 (24.96)	30.72 (19.53)	
Letter cancellation (left omissions)	10.25 (7.63)	4.62 (6.09)	7.83 (11.29)	7.00 (9.63)	
Gainotti drawing (max 6)	4.50 (1.07)	5.20 (1.00)	4.33 (1.21)	4.83 (1.33)	
Reading task (max 116)	8.50 (12.75)	3.00 (3.82)	16.00 (35.78)	16.00 (37.24)	
Line bisection (rightward deviation, mm)	20.08 (22.43)	8.35 (15.87)	16.04 (28.89)	10.23 (25.27)	
Daisy drawing (max 3)	2.00 (0.92)	2.62 (1.06)	1.33 (0.82)	1.50 (0.84)	
Landmark task ("left shorter" answers, max 12)	8.00 (3.78)	7.5 (3.74)	8.00 (3.29)	9.00 (3.29)	

Table 2: Grey matter clusters showing decreased cortical thickness associated with poor recovery after PA therapy

GM clusters	MNI coordinates			CS	Corrected *P*	Effect size *d*
	x	*y*	*z*			
1. L perisylvian regions	-43	-3	-21	31947	0.037	0.26
2. L Temporo-parietal junction	-48	-55	15	1539	0.048	0.67
Angular g						
Middle temporal lobe						
3. L Temporal lobe	-33	-16	-32	670	0.049	1.24
ITg						
L fusiform g						
Parahippocampal g						

CS, cluster size (i.e., number of voxels); L, left; g, gyrus; ITL, inferior temporal gyrus; IPL, inferior parietal lobule.

Grey matter clusters significantly associated with poor recovery of neglect after prism adaptation (P_{TFCE}<0.05). Coordinates indicate the location of the cluster peak in Montreal Neurological Institute (MNI) convention.

Table 3: White matter clusters showing decreased fractional anisotropy FA (P_{TFCE}<0.05) in the low-responder group as compared with the high-responder group

WM clusters	MNI coordinates			CS	Corrected *P*	Effect size *d*
	x	*y*	*z*			
1. CC body	2	-20	24	1533	0.019	1.57
2. CC genu	0	24	0	47	0.049	1
3. L CC genu	-12	31	-2	9	0.049	0.85

CS, cluster size (i.e., number of voxels); CC, corpus callosum; L, left.

Coordinates indicate the location of the cluster peak in Montreal Neurological Institute (MNI) convention.

Figure legends

Figure 1: Patients' grey matter lesion anatomy. (1) Overlap of the lesions for all the included right brain-damaged patients for each group. (2) Results of the subtraction of the probability map of the high-recovery group from the probability map of the low-recovery group.

Figure 2: Relationship between cortical thickness and recovery rate score represented by the four clusters. Results are represented at $p<0.05$ and corrected for multiple comparisons.

Figure 3: Results of TBSS between-groups comparisons represented by the three clusters. FA differences ($p<0.05$) are represented in red.

Figure 4: Percentage maps in healthy subjects (BCB toolkit (http://www.brainconnectivitybehaviour.eu) showing the cortical projections of the voxels identified by TBSS analysis in low recovery patients compared to high-recovery patients.

Fig. 1

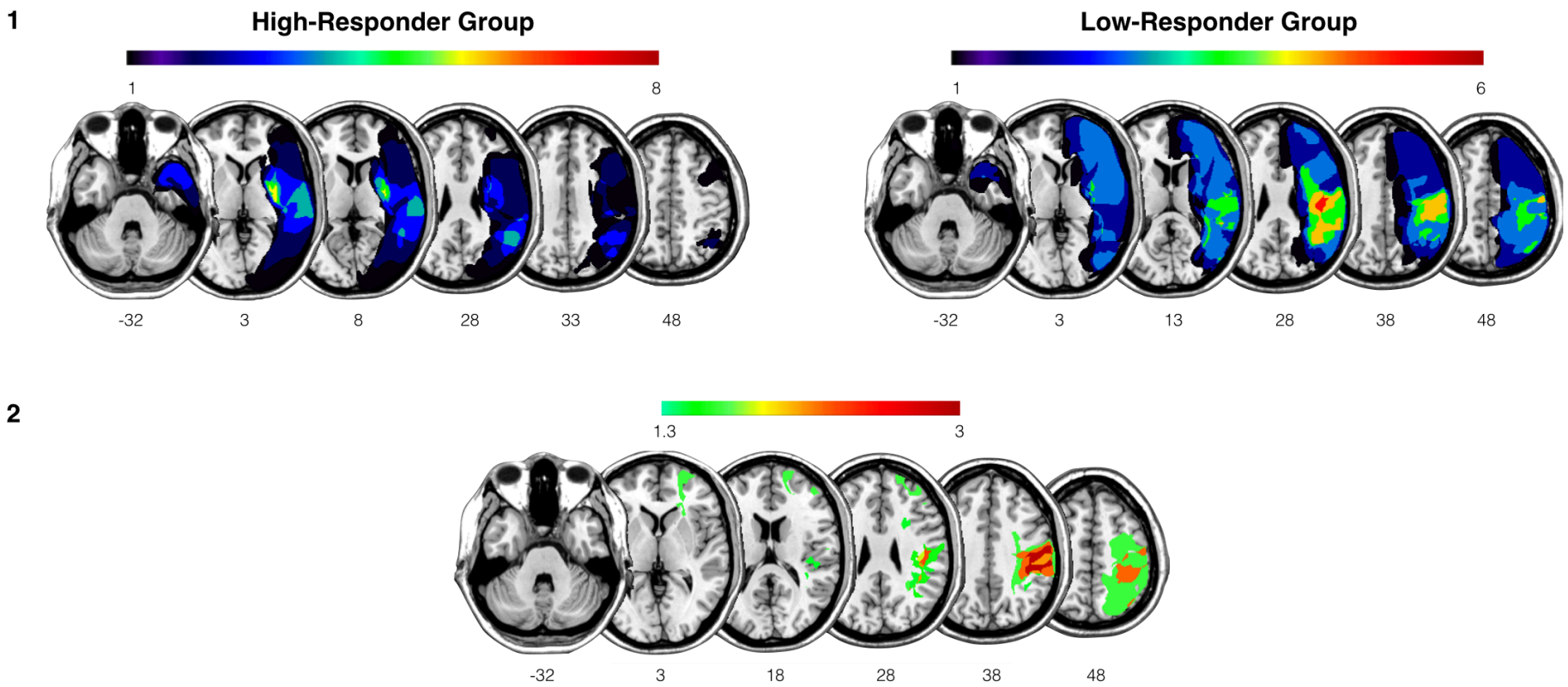
1
High-Responder Group
1
8
-32
3
8
28
33
48
Low-Responder Group
1
6
-32
3
13
28
38
48
2
1.3
3
-32
3
18
28
38
48

Fig. 2

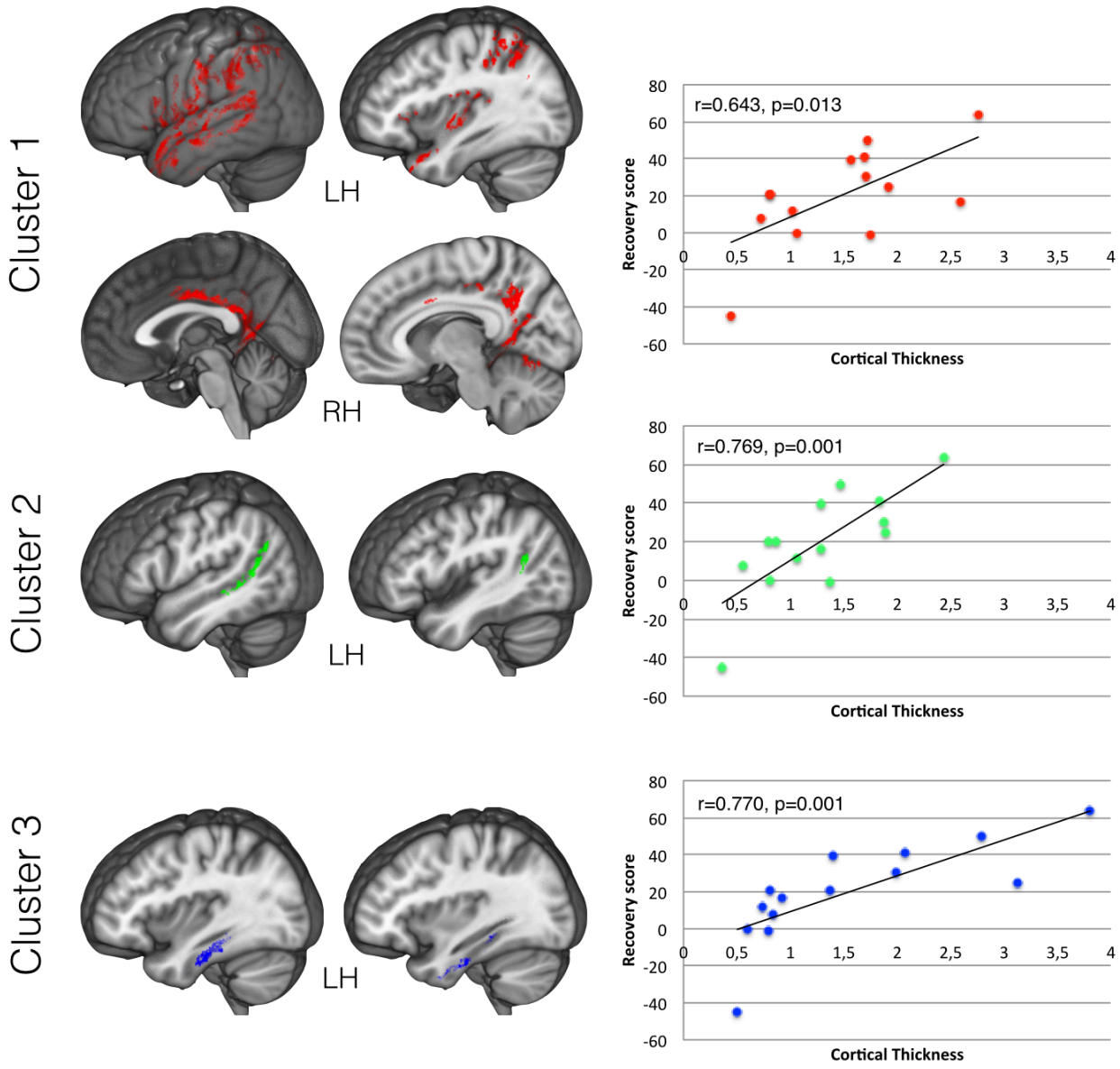
Cluster 1
LH
RH
r=0.643, p=0.013
Recovery score
Cortical Thickness
Cluster 2
LH
r=0.769, p=0.001
Recovery score
Cortical Thickness
Cluster 3
LH
r=0.770, p=0.001
Recovery score
Cortical Thickness

Fig. 3

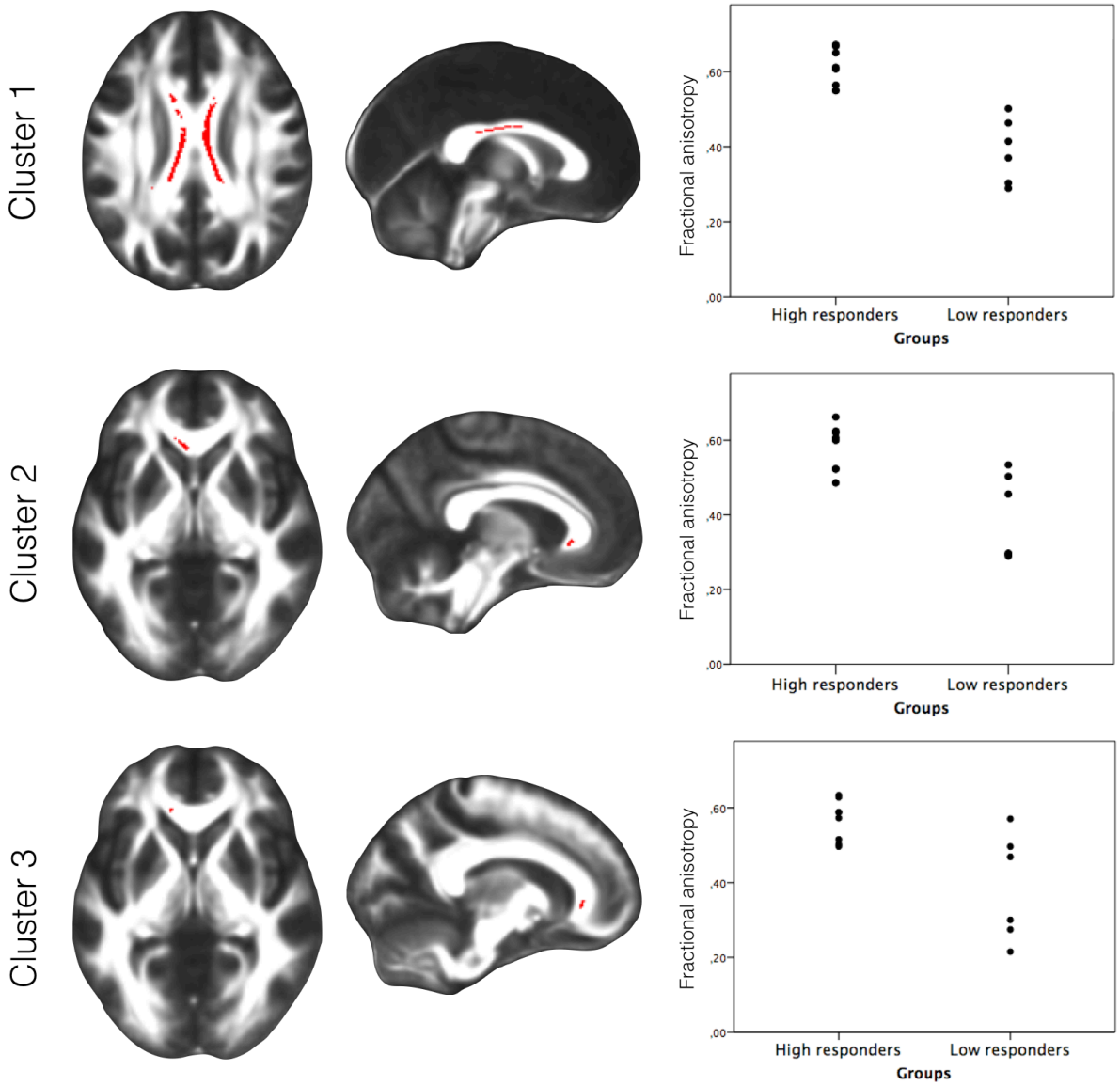
Cluster 1
Cluster 2
Cluster 3
Fractional anisotropy
,00
,20
,40
,60
High responders
Low responders
Groups
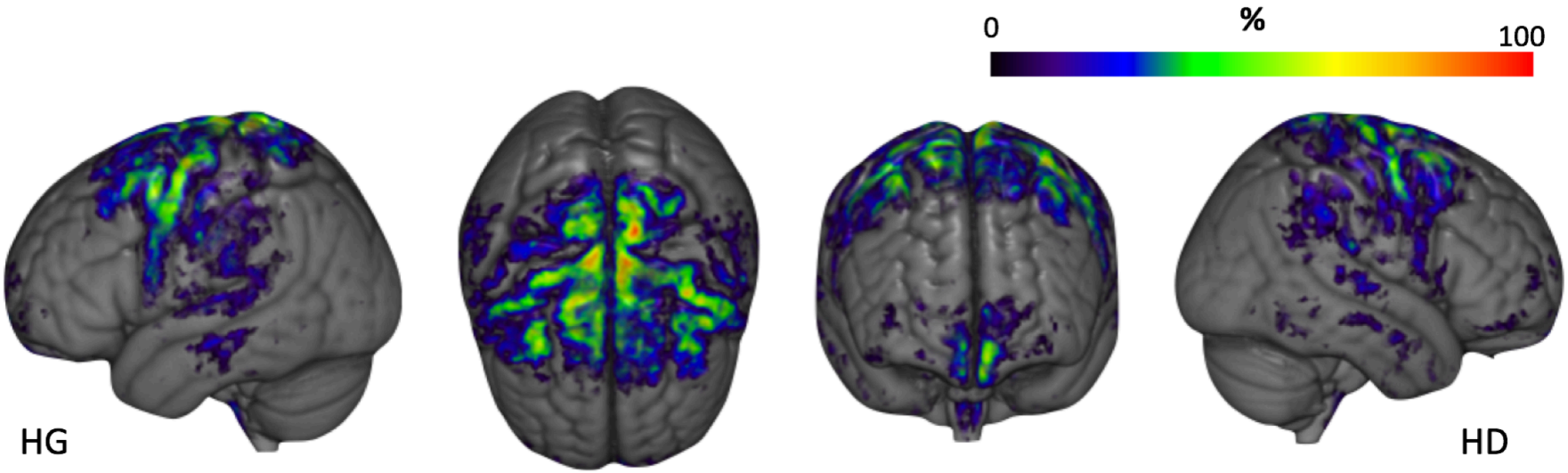
Fig. 4